Revised MS 27672

ROLE OF ENDOGENOUS XAP2 PROTEIN ON THE LOCALIZATION AND NUCLEOCYTOPLASMIC SHUTTLING OF THE ENDOGENOUS MOUSE Ah^{b-1} RECEPTOR IN THE PRESENCE AND ABSENCE OF LIGAND

Richard S. Pollenz, Sarah E. Wilson and Edward J. Dougherty

From the Department of Biology, University of South Florida, Tampa, FL, 33620

Running Title: Role of XAP2 in Endogenous Ah^{b-1} AHR Function

Corresponding Author: Richard S Pollenz, University of South Florida, Department of Biology, BSF 110, 4202 E Fowler Ave, Tampa, FL 33620, Tel. 813-974-1596, Fax. 813-974-3263, E-Mail:pollenz@cas.usf.edu

Text Pages = 18

Tables = 0

Figures = 7

References = 33

words in abstract = 248

words in Intro = 694

words in Disc. = 1206

Abbreviations: XAP2, hepatitis B virus X-associated protein AHR, Ah receptor; GAR-HRP, goat-anti rabbit horseradish peroxidase; GAM-HRP, goat-anti mouse horseradish GAR-RHO, peroxidase; goat anti rabbit IgG conjugated to rhodamine; BSA, bovine serum albumen; PBS, phosphate buffered saline; siRNA, small interfering RNA; TCDD, 2,3,7,8-tetrachlorodibenzo-p-dioxin; LA-I, Hepa-1 variant cell line with reduced AHR; AH_{WT}, stable LA-I Hepa-1 cells expressing the Ah^{b-1} receptor; AH_{500}, stable LA-I Hepa-1 cells expressing the Ah^{b-1} receptor truncated at amino acid 500; AH_{640}, stable LA-I Hepa-1 cells expressing the Ah^{b-1} receptor truncated at amino acid 640. ECL, enhanced chemiluminescence (ECL).

ABSTRACT

Studies using transient expression systems have implicated the hepatitis B virus X-associated protein (XAP2) in the control of aryl hydrocarbon receptor (AHR) stability and subcellular location. Studies were performed in Hepa-1 cells to evaluate these functions of XAP2 on the mouse Ah^{b-1} receptor under endogenous stoichiometry. The Ah^{b-1} receptor is cytoplasmic and it becomes predominantly nuclear after 30-60 minutes of ligand exposure with minimal degradation. During this time, XAP2 co-precipitates with the AHR suggesting that it does not impact the nuclear localization of the liganded receptor. Over-expression of XAP2 in Hepa-1 cells does not result in increased association with the endogenous Ah^{b-1} complex or influence the receptors cytoplasmic localization. Knock down of endogenous XAP2 by siRNA results in ≥90% reduction in the amount of XAP2 associated with the endogenous Ah^{b-1} receptor complex. Despite the reduction in XAP2, the unliganded Ah^{b-1} receptor complex remains cytoplasmic, although inhibition of nuclear export results in accumulation of the receptor in the nucleus. Truncation of the C-terminal 305 amino acids of the Ah^{b-1} receptor (AHR_{500}) results in proteins that exhibit a predominantly nuclear localization and remain associated with the same level of endogenous XAP2 as full length AHRs. Collectively, these results support a model in which the majority of the unliganded Ah^{b-1} receptor complexes are associated with XAP2 and the association prevents dynamic nucleocytoplasmic shuttling in the unliganded state. Following ligand binding, XAP2 remains associated with the Ah^{b-1} receptor complex and does not impair nuclear translocation but may function to limit receptor “transformation”.

The hepatitis B virus X-associated protein, XAP2 (also termed ARA9 and AIP) was identified as a component of the latent aryl hydrocarbon receptor (AHR) complex using yeast two-hybrid screens and direct immunoprecipitation (Carver et al., 1997; Ma and Whitlock 1997; Meyer et al., 1998). XAP2 shares sequence identity with the FKBP52 class of immunophilins and this class of proteins is involved in subcellular trafficking, stability and transactivation potential of steroid hormone receptors (reviewed in Petrulis and Perdew 2002; Davis and Sanchez 2005). Interestingly, it has recently been determined that individuals with pituitary adenoma predisposition (PAP), carry germline mutations within the XAP2 gene (Vierimaa et al., 2006). The mechanism of how loss of function of XAP2 results in PAP and the possible relationship to the AHR is currently unclear, however, these findings highlight the importance of XAP2 and its associated proteins in normal cellular physiology.

Since XAP2 shares sequence identity with FKBP52, several studies have evaluated the function XAP2 with regard to the subcellular trafficking, stability and transactivation potential of the AHR. However, with few exceptions, the analysis of AHR and XAP2 interactions has been carried out *in vitro* or in transient expression systems utilizing the Ah^{b-1} receptor that is expressed in the C57BL/6 strain of mouse. The results of these studies suggest that overexpression of XAP2 increases the level of Ah^{b-1} receptor protein and enhances the level of AHR-mediated gene regulation (Carver et al., 1997; Ma and Whitlock 1997; Meyer and Perdew 1999; Bell and Poland 2000; Meyer et al., 2000; LaPres et al., 2000). In addition, it has been reported that XAP2 expression can impact the subcellular localization of the Ah^{b-1} receptor and prevents it from undergoing dynamic nucleocytoplamsic shuttling in COS and HeLa cell lines (Kazlauskas et al., 2000; Kazlauskas et al., 2002; Petrulis et al., 2002; Berg and Pongratz 2002). Although these findings are consistent with the function of immunophilin-like proteins in other receptor-mediated pathways (Davis and Sanchez 2005), there is increasing evidence

that the contribution of XAP2 to AHR function may be specific to the Ah^{b-1} class of receptors and needs to be evaluated in an endogenous context.

To evaluate the role of endogenous XAP2 with different species of AHRs, studies were recently completed in cell lines that expressed endogenous mouse Ah^{b-1}, Ah^{b-2} and rat AHRs and contained similar levels of endogenous XAP2 (Pollenz and Dougherty 2005). Importantly, the unliganded mouse Ah^{b-2} and rat AHR complexes were associated with greatly reduced levels of XAP2 when compared to Ah^{b-1} receptors. In addition, mouse Ah^{b-2} and rat AHR complexes exhibited dynamic nucleocytoplasmic shuttling in the absence of exogenous ligands and the mouse Ah^{b-2} and rat AHRs exhibited a greater magnitude of ligand-induced degradation than Ah^{b-1} receptors. When the mouse Ah^{b-2} receptor was stably expressed in the C57BL/6 background, it was associated with minimal levels of XAP2, showed dynamic nucleocytoplasmic shuttling and exhibited increased levels of ligand-induced degradation. Similar results have been reported for the human AHR, where the expression of XAP2 has been shown to have little impact on the subcellular localization or expression level of the receptor (Ramadoss et al., 2004). Collectively, these results demonstrate that there are striking differences in how XAP2 impacts AHR-mediated signal transduction across species lines and suggest that endogenous XAP2 may function to modulate subcellular location and stability of only the Ah^{b-1} receptor complex. Since the concentration and subcellular locations of signaling proteins are critical parameters in their functionality, there are several key issues that need to be resolved with regard to XAP2 function on AHR-mediated signaling. First, it has not yet been determined whether XAP2 remains associated with the endogenous Ah^{b-1} receptor after ligand binding and nuclear translocation. Second, it is unclear whether the localization of the Ah^{b-1} receptors within the cytoplasm is solely dependent on its association with XAP2. Finally, it is of interest to investigate whether the reduced level of nucleocytoplasmic shuttling of the Ah^{b-1} receptor is due to its

association with XAP2. The analysis of these questions will be important in further understating role of XAP2 in the response of the AHR to toxicologically relevant chemicals as well as refining the mechanisms involved in ligand-induced degradation and gene regulation.

MATERIALS AND METHODS

Materials

TCDD (98% stated chemical purity) was obtained from Radian Corp. (Austin, TX) and was solubilized in dimethylsulfoxide (me_2SO). Geldanamycin (GA), leptomycin B (LMB) were purchased from Sigma (St. Louis, MO). pC3-NLS-GFP-GST-RevNES was a generous gift from Dr. Roland Stauber (Georg-Dpeyer-Haus, Germany). pCI-hXAP2 and pEYFP-XAP2-FLAG were generously provided by Dr. Gary Perdew (Penn State University).

Antibodies

Specific polyclonal antibodies against either the AHR (A-1, A-1A) or ARNT protein (R-1) are identical to those described previously (Pollenz et al., 1994; Holmes and Pollenz 1997). Antibodies to XAP2 (Novus, Littleton, CO), actin (Sigma), and rat P4501A1 (Chemicon Intl. Temecula, CA) were purchased from commercial sources. For western blot analysis goat anti rabbit or anti mouse antibodies conjugated to horseradish peroxidase (GAR-HRP, GAM-HRP) were utilized. For immunohistochemical studies, goat anti rabbit IgG conjugated to rhodamine (GAR-RHO) were used. Both of these reagents were purchased from Jackson Immunoresearch (West Grove, PA).

Buffers

PBS is 0.8% NaCl, 0.02% KCl, 0.14% Na_2HPO_4, 0.02% KH_2PO_4, pH 7.4. SDS sample buffer buffer is 60mM Tris, pH 6.8, 2% SDS, 15% glycerol, 2mM EDTA, 5mM EGTA 10mM DTT, 0.005% bromphenol blue. Lysis buffer buffer is 60mM Tris, pH 6.8, 2% SDS, 15% glycerol, 2mM EDTA, 5mM EGTA 10mM DTT, 0.5% NP-40, 20mM sodium molybdate 0.005% bromphenol blue. RIPA is 50mM Tris, 150mM NaCl, 0.2% NP-40, 20mM sodium molybdate, 20mM DL-histidine, pH 7.4. TTBS is 50mM Tris, 0.2% Tween 20, 150mM NaCl, pH 7.5. TTBS+ is 50mM Tris, 0.5% Tween 20, 300mM NaCl, pH 7.5. BLOTTO is 5% dry milk in TTBS.

Cells and Growth Conditions

Wild type Hepa-1c1c7 (Hepa-1), and type I (LA-I) Hepa-1 variants were a generous gift from Dr. James Whitlock, Jr. (Department of Pharmacology, Stanford University). LA-I cells stably expressing truncated AHR were produced as detailed (Pollenz et al., 2005). Wild type Hepa-1 cells were propagated in DMEM supplemented with 10% fetal bovine serum (FBS). Stable lines were propagated in DMEM supplemented with 10% FBS and 400ug/ml G418. All cell lines were passaged at 1-week intervals and used in experiments during a 3-month period at approximately 70%-90% confluence. For treatment regimens, stated concentrations of TCDD, GA or LMB were administered directly into growth media for the indicated incubation times.

Preparation of total cell lysates

Following treatment, cell monolayers were washed twice with PBS and detached from plates by trypsinization (0.05% trypsin/0.5mM EDTA). Cell pellets were washed with PBS and sonicated directly in 75-150µl ice-cold lysis buffer for 12 seconds. Lysates were immediately heated for 3 min at 100^{o}C and then sonicated an additional 5 seconds. Samples were stored at -20^{o}C until analysis.

Preparation of cytosol and immunoprecipitation

Cells were harvested by trypsinization as described above and disrupted by vortexing in RIPA buffer supplemented with PMSF (10mM), and aprotinin (10µM). Cytosol was generated by centrifugation at 30,000 x g used for immunoprecipitation studies without prior freezing. Protein concentrations were determined using the Commassie Plus assay (Pierce, Rockford, IL) with BSA as the standard. Typically, immunoprecipitations were carried out with 600µg of cytosol in a total of 600µl of RIPA buffer supplemented with BSA (20µg/ml) and histidine (20mM). Triplicate samples were incubated with either affinity pure A1-A (AHR) IgG (5µg) or affinity pure pre-immune (Pi) rabbit IgG (5µg) for 90 minutes at 4^{o}C. 25µl Protein A/G agarose (Pierce) was added

and the incubation continued an additional 90 minutes at 4^{o}C. Pellets were washed with TTBS containing sodium molybdate (20mM) three times for 5 min at 4^{o}C and protein eluted by boiling in 30µl SDS sample buffer. Samples were then centrifuged at 30,000 x g, and the triplicate samples combined. 15-20µl of sample was then resolved by discontinuous polyacrylamide slab gels (SDS-PAGE) and blotted to nitrocellulose. Due to the large amount of total protein needed for each IP experiment, it was not possible to do duplicate samples. However, all IP studies were repeated at least two times.

Western blot analysis and quantification of protein

Equal amounts of protein were resolved by SDS-PAGE and electrophoretically transferred to nitrocellulose. Immunochemical staining was carried out with varying concentrations of primary antibody (see text and figure legends) in BLOTTO buffer supplemented with DL-histidine (20mM) for 1-2 hours at 22^{o}C. Blots were washed with 3 changes of TTBS+ for a total of 45 minutes. The blot was incubated in BLOTTO buffer containing a 1:10,000 dilution of appropriate peroxidase conjugated secondary antibody for 1 hour at 22^{o}C and washed in 3 changes of TTBS+ as above. Prior to detection, the blots were rinsed in PBS. Bands were visualized with the enhanced chemiluminescence (ECL) kit as specified by the manufacturer (GE/Healthcare, Piscataway, NJ). Multiple exposures of each set of samples were produced. The relative concentration of target protein was determined by computer analysis of the exposed film as detailed previously (Pollenz 1996; Holmes and Pollenz 1997; Pollenz et al., 1998).

Immunofluorescence staining and microscopy

All immunocytochemical procedures (cell plating, fixation, and staining) were carried out as previously described (Pollenz et al., 1994; Pollenz 1996; Holmes and Pollenz 1997). Cells were observed on an Olympus IX70 microscope. On average, 5-10 fields (15-25 cells per field) were evaluated on each coverslip and 3-4 fields were photographed with a digital camera at the same exposure time to generate the raw data.

Nuclear fluorescence intensities of 50-75 cells in 3-4 distinct fields of view, were obtained using MicroSuite image analysis software (Olympus America Inc.).

Transfection and RNA interference

Annealed small interfering RNA (siRNA) complexes containing 21bp regions of identity to regions of the murine XAP2 or an annealed 21bp RNA to sequence not present in the mouse genome (siCON) were purchased from Ambion (Austin, TX). siRNA (final concentration of 50-100nM) or plasmid DNA (1µg/well) was transfected into 35mm dishes containing 1-2 x 10^5/cells using lipofectamine™ reagent (Invitrogen, Carlsbad, CA). To monitor transfection efficiency, the BLOCK-IT® FITC labeled RNA reagent (Invitrogen) was included in the transfection cocktail. 24-48 hours after transfection, cells were treated as detailed in the text and total cell lysates harvested for Western blotting or the cells fixed and stained as detailed above. The efficiency of siRNA gene knock down of XAP2 was determined by Western blotting. Transfection efficiency was monitored by microscopy using FITC labeled RNA (Clontech). In general, transfection efficiency in all experiments was >85%.

Statistical analysis

Target protein bands from total cell lysates were normalized to internal standards (actin) to generate normalized densitometry units. Target protein values or nuclear fluorescence intensities were compared by ANOVA and Tukey-Kramer multiple comparison tests using InStat software (GraphPad Software Inc. San Diego, CA). Results are presented as mean $\pm$ SE. A probability value of <0.05 was considered significant.

RESULTS

XAP2 remains associated with the Ah^{b-1} AHR complex after ligand binding and nuclear translocation

Studies using transient expression experiments suggest that XAP2 functions in AHR-mediated signal transduction by stabilizing the latent AHR complex and modulating subcellular localization (Carver et al., 1997; Ma and Whitlock 1997; Meyer and Perdew 1999; Bell and Poland 2000; Meyer et al., 2000; LaPres et al., 2000; Kazlauskas et al., 2000; Kazlauskas et al., 2002; Petrulis et al., 2002; Berg and Pongratz 2002). However, the function that XAP2 exerts on nuclear translocation of the endogenous Ah^{b-1} AHR following ligand binding remains to be resolved. To begin to address this question, it is first necessary to determine the precise time line of nuclear localization and degradation of the endogenous Ah^{b-1} AHR following ligand exposure. Hepa-1 cells were treated with TCDD for 0-300 minutes and the endogenous Ah^{b-1} AHR visualized by immunocytochemistry or quantified in total cell lysates using Western blotting. The time course of nuclear localization is presented in Figure 1A. In untreated cells (time =0) it can be observed that the endogenous Ah^{b-1} AHR is localized predominately within the cytoplasmic compartment. Following 30-45 minutes of ligand stimulation, the fluorescence intensity associated with the AHR becomes predominantly nuclear and then declines (Figure 1A). These results are in agreement with previous analyses of the endogenous Ah^{b-1} AHR as well as studies that have assessed the localization of AHR-GFP chimeras (Pollenz et al., 1994; Pollenz 1996; Davarinos and Pollenz 1999; Song and Pollenz 2002; Pollenz and Dougherty 2005; Elbi et al., 2002).

To obtain a quantitative measure of the change in AHR localization, image analysis was used to measure the relative fluorescence intensities of the Hepa-1 nuclei. The average values for 75-100 individual cells were then plotted as a function of time and a representative experiment is shown in Figure 1B. The results indicate that the

fluorescence intensity of the nucleus peaks 45-60 minutes after ligand stimulation and then declines over the remaining time frame to levels at or below those of the time = 0 cells. Since there is no recovery of the fluorescence to other cellular compartments throughout the time course, these results are consistent a nuclear translocation event that is followed by degradation. To validate this hypothesis, quantitative Western blotting was carried out on total cell lysates that were prepared from Hepa-1 cells exposed to TCDD over the identical time frame shown in Figure 1A. A representative Western blot is shown in Figure 1C and the quantified results are presented in Figure 1B. As expected, the overall level of AHR protein is reduced by approximately 82% after 240-300 minutes of TCDD exposure, but the key finding of these studies is that the degradation of the AHR does not occur immediately following ligand exposure. Indeed, the level of AHR declines by only 20% during the first 75 minutes of ligand exposure with the majority of the AHR protein degraded between the 75-240 minute time points. Importantly, the time course of AHR degradation paralleled the reduction that was observed in the nuclear fluorescence. These results establish that during the first 60-75 minutes of ligand exposure, the Ah^{b-1} receptor protein is translocated to the nuclear compartment without undergoing high levels of degradation. Therefore, the first 60-75 minutes of ligand exposure provides a window of time for the analysis of changes within the endogenous Ah^{b-1} receptor complex that will not be confounded by large reductions in the basal level of the protein.

The next series of studies were designed to assess the association of XAP and ARNT with the soluble AHR complex during the first 75 minutes of ligand exposure. Hepa-1 cells were stimulated with TCDD for 0-75 minutes, harvested and then lysed by vortexing in buffer containing non-ionic detergent. The supernatant fractions were incubated with antibodies specific to the AHR and these complexes precipitated with Protein A-G agarose as described in *Materials and Methods*. Identical samples were

then evaluated for level of XAP2, AHR and ARNT by Western blotting. Cell disruption by this method has been found to be sufficient to allow redistribution of soluble proteins from the nucleus (Paine et al., 1983; Pollenz et al., 1994; Holmes and Pollenz 1997), thus, any AHR that was translocated to the nucleus but was not tightly associated with nuclear structures should partition to the supernatant fraction and be available for immunoprecipitation. This study was carried out three times and a representative experiment is shown in Figures 2A and 2B.

The results show that AHR, XAP2 and ARNT are present in all of the supernatant fractions and that the AHR can be specifically precipitated from each. Importantly, XAP2 is co-precipitated from all of the fractions while ARNT co-precipitates from the fractions prepared from cells that were exposed to ligand for 20, 40, 60 and 75-minutes. Since the results in Figure 1 clearly show that the AHR is predominately nuclear after 45 minutes of ligand exposure, these findings suggest that there are multiple pools of soluble AHR complexes in the nucleus of the Hepa-1 cell after ligand exposure and that some of the complexes remain associated with XAP2. To determine whether there were differences in the relative ratio of XAP2:AHR at each time point, the blots presented in Figure 2A were quantified by densitometry and the results are presented in Figure 2B. The results show that over the time course of study, the level of AHR is reduced by approximately 20% while the level of XAP2 that is co-precipitated is reduced by approximately 40% between the 40-75 minute time points. Thus, a portion of the XAP2 is being lost from the AHR complex over time. However, the level of ARNT that is co-precipitated increases over the time course. This type of trend suggests a model in which the soluble AHR complex not associated with XAP2 is associated with ARNT. It is important to note however, that even though the level of XAP2 associated with the AHR core complex is declining during the time course XAP2 remains associated with a significant proportion of the AHR complex even after 75 minutes of ligand exposure.

Figure 1C shows that the endogenous Ah^{b-1} receptor is not fully degraded following ligand exposure and a small fraction of receptors (15-20%) remains in the cells six hours later. Similar results have been reported in cells treated with ligands for 24-48 hours and beyond (Giannone et al., 1995; Pollenz 1996; Pollenz et al., 1997). These findings are in contrast to those in cell lines expressing endogenous Ah^{b-2} or rat AHRs where the AHR is degraded by 95-100% following only 2-4 hrs of ligand exposure (Pollenz 1996; Davarinos and Pollenz 1999; Pollenz and Dougherty 2005). Thus, it was pertinent to determine whether XAP2 was associated with the population of Ah^{b-1} receptors that remained in Hepa-1 cells following prolonged ligand exposure. Hepa-1 cells were treated with TCDD for 4 hours and supernatant fractions prepared. The results show that the level of endogenous AHR in the input fraction prepared from the TCDD-treated cells is reduced by approximately 85% (Figure 2C). The samples were then immunoprecipitated with the following modification: 7-fold more sample protein was used to precipitate the AHR from the TCDD-treated samples compared to the controls while the overall volume and amount of AHR IgG used in the experiment was held constant. This modification allowed the overall level of AHR being precipitated to be equal between the two samples. The results show that under these experimental conditions, nearly equal levels of AHR were precipitated from each fraction and a comparatively equal amount of XAP2 was also co-precipitation from each sample (Figure 2C). Thus, the relative ratio of XAP2:AHR was the same in both the control and TCDD-treated samples (Figure 2D). Therefore, these findings suggest that there is a small population of Ah^{b-1} receptors that are recalcitrant to the ligand induced degradation events and they remain associated with XAP2.

Exogenous expression of XAP2 does not affect the localization of the *endogenous Ah^{b-1} AHR complex or the level of XAP2 associated with the Ah^{b-1} AHR complex*

Previous results suggest that the entire pool of Ah^{b-1} receptor complexes in Hepa-1 cells is not associated with XAP2 and that there are populations of receptors that reside in the nucleus (Petrulis et al., 2000). Thus, based on these results, it would be predicted that expression of exogenous XAP2 in the Hepa-1 line would result in increased association of XAP2 with the endogenous Ah^{b-1} receptor complex, increased distribution of the complex to the cytoplasm and possibly increased levels of AHR protein. Thus, Hepa-1 cells were transfected with vectors that express either human XAP2 (hXAP) or yellow fluorescent protein tagged hXAP (YFP-XAP2). Following 24 hrs, total cells lysates were prepared and evaluated by Western blotting or cells fixed and stained to assess the localization of the endogenous AHR. The hXAP constructs used for these studies have been shown to interact with the mAHR and influence its subcellular localization and expression level in transient transfection assays (Meyer et al., 2000; Petrulis et al., 2000; Ramadoss et al., 2004). Figure 3A shows that the overall level of total XAP protein can be elevated 3-4 fold when Hepa-1 cells are transfected with vectors that express hXAP or YFP-XAP2 and that the increased level XAP2 protein does not result in an elevation in the concentration of the endogenous Ah^{b-1} receptor. To determine if the increased level of XAP2 expression influenced the subcellular localization of the unliganded Ah^{b-1} receptor, transfected cells were stained for the AHR. Representative images are shown in Figure 3B. As shown in Figure 1, the endogenous Ah^{b-1} receptor exhibited a predominantly cytoplasmic staining pattern, and populations expressing increased levels of XAP2 showed no significant changes in this pattern. Importantly, the inability to observe changes in the subcellular localization of the endogenous Ah^{b-1} complex was not due to low levels of transfection efficiency since >85% of the population showed an FITC signal from the tagged RNA that was included

in the transfection cocktail. In addition, the cytoplasmic localization of the Ah^{b-1} receptor is unaltered in cells that express YFP-XAP2 when compared to cells that were not transfected (Figure 3B). Thus, these results show that increased expression of hXAP2 in Hepa-1 cells does not impact the concentration or localization of the endogenous Ah^{b-1} receptor.

Since the increased expression of hXAP did not appear to influence the subcellular location of the endogenous Ah^{b-1} receptor, it was pertinent to determine whether increased expression of hXAP resulted in an increase in the level of total XAP2 associated with the Ah^{b-1} complex. Therefore, transfected cells were lysed, the AHR complex immunoprecipitated with AHR antibodies and the samples evaluated for AHR and XAP2 protein by Western blotting. This study was carried out two times and a representative experiment is presented in Figure 4A and the quantified results presented in Figure 4B. In the study presented, the level of hXAP overexpression was approximately 3.5-fold above the level of endogenous mXAP2 and the hXAP can be distinguished from the endogenous mXAP2 since it resolves at a slightly lower molecular mass. Importantly, when hXAP was expressed in the Hepa-1 cells, both hXAP and mXAP2 were co-precipitated with the AHR. However, despite the increased level of total XAP2 protein that was present in the transfected population, the level of associated hXAP did not increase the total amount of XAP2 associated with the AHR complex, but replaced a similar amount of endogenous mAXP2 (Figure 4A, B). Thus, the total amount of XAP2 associated with the endogenous AHR complex was not elevated above the level found in control cells (note that the relative ratio of total XAP2:AHR in the four samples is essentially the same). Collectively, these results support the hypothesis that the entire population of endogenous Ah^{b-1} complex in Hepa-1 cells is associated with XAP2.

Reduction of endogenous XAP2 with siRNA does not affect the localization of the endogenous Ah^{b-1} complex but stimulates its nucleocytoplasmic shuttling.

The previous results suggest that the entire population of Ah^{b-1} complex is associated with XAP2 and that under endogenous stoichiometry the XAP2 protein remains associated with the Ah^{b-1} receptor after the ligand-induced nuclear translocation event. Thus, it was pertinent to assess whether the cytoplasmic localization of the unliganded Ah^{b-1} complex and its inability to undergo dynamic nucleocytoplasmic shuttling was due to its association with XAP2. The strategy for these studies was to reduce the level of endogenous XAP2 protein by transfection of siRNAs specific to XAP2 and then assess the localization of the AHR by immunocytochemistry. However, it was first necessary to demonstrate that the siRNA protocol would lead to a reduction in the level of XAP2 actually *associated* with the endogenous AHR complex and also establish conditions to inhibit nucleocytoplasmic shuttling in the Hepa-1 cell line.

To establish that endogenous AHR complexes could be generated that were associated with reduced level of XAP2, Hepa-1 cells were transfected with control (siCON) or XAP2-specific (siXAP2) siRNA as detailed in Materials and Methods and allowed to recover for 48 hrs. Supernatant fractions were prepared from the transfected cells and immunoprecipitation studies carried out as described previously. A representative experiment is shown in Figure 4A. The input samples demonstrate that Hepa-1 cells transfected with siXAP2 exhibit >80% reduction in the level of endogenous XAP2 compared to cells transfected with siCON. When the AHR was immunoprecipitated from these samples, the amount of XAP2 associated with the endogenous AHR complex was reduced by >90% in comparison to controls (Figure 5A, B). Thus, these studies confirm that reductions in the basal levels of XAP2 are reflected in equal or greater reductions in the level of XAP2 associated with the unliganded AHR core complex.

It was next important to determine conditions to inhibit nucleocytoplasmic shuttling behavior in the Hepa-1 cell line. For these studies Hepa-1 cells were transfected with the pC3-NLS-GFP-GST-RevNES expression construct that expresses a chimeric GFP-GST fusion protein containing both nuclear localization (NLS) and nuclear export (NES) sequences (Knauer et al., 2005). Cells were then treated with vehicle control or leptomycin B (1nM) for two hrs to inhibit CRM-1 mediated nuclear export (Kudo et al., 1997; Kudo et al., 1998). The location of the GFP was monitored by fluorescence microcopy and representative photographs are shown in Figure 5C. Interestingly, the GFP chimera exhibited a predominantly cytoplasmic localization in the untreated Hepa-1 line despite the presence of both NLS and NES domains (Figure 5C, control). In contrast, when Hepa-1 cells were treated with LMB, the GFP chimera became rapidly localized within the nuclear compartment (Figure 5C, LMB). Thus, these experiments establish that proteins can undergo rapid nucleocytoplasmic shuttling behavior in the Hepa-1 line, and that the process can be efficiently inhibited by using 1nM LMB.

Having established conditions to reduce the level of XAP2 associated with the core AHR complex and also inhibit nuclear export, studies were designed to assess whether a reduction in XAP2 would affect the shuttling behavior of the endogenous AHR. Hepa-1 cells were transfected with siCON or siXAP2 as well as marker RNA tagged with FITC to monitor transfection efficiency. 48 hours later, cells were treated with 1nM LMB or vehicle control for 4 hrs and then fixed and stained for AHR. In addition, several duplicate plates of cells were used to generate total cell lysates so that the level of AHR and XAP2 protein could be evaluated by Western blotting. A representative experiment is shown in Figure 6. The Western blot results confirm that the level of endogenous XAP2 was reduced by >80% in cells transfected with siXAP2 (Figure 6A). Strikingly, reductions in XAP2 do not appear to affect the distribution of the

unliganded AHR complex (Figure 6B). Indeed, cells with reduced XAP2 show the same cytoplasmic distribution of the AHR as cells transfected with control siRNA. In contrast, there is a marked increase in the nuclear localization of the AHR when cells transfected with siXAP2 are treated with LMB for 4 hrs. The change in localization of the AHR is not observed in LMB treated cells transfected with siCON. It is important to note that the transfection efficiency in the experiment presented in Figure 6 was approximately 90% and is illustrated by the high number of cells that are labeled with the FITC tagged RNA used to monitor transfection. Collectively, these results suggest that when endogenous XAP2 is reduced in the Hepa-1 cell line, the endogenous Ah^{b-1} receptor undergoes a moderate level of nucleocytoplamsic shuttling yet retains a predominantly cytoplasmic localization.

Truncation of the C-terminal portion of the Ah^{b-1} AHR results in constitutively nuclear AHR that is associated with XAP2

To gain additional insight into the role that the endogenous XAP2 plays in the subcellular location of the AHR, stable cell lines were generated that expressed Ah^{b-1} receptors that carried C-terminal truncations (Figure 7A). These cell lines have been described previously (Pollenz et al., 2005) and are useful for the analysis of XAP2 function on nuclear translocation since the truncated AHRs show distinct subcellular localization. Figure 7B shows the localization of AHR_{WT}, AHR_{500} and AHR_{640} in cells that have been fixed and stained with AHR antibodies. It can be observed that AHR_{500} is localized predominately within the nucleus in the absence of exogenous ligand while AHR_{WT} and AHR_{640} show the expected cytoplasmic localization. To confirm that the nuclear localization of AHR_{500} was not an artifact of integration events during construction of the cell line, six independent lines were evaluated and all exhibited the nuclear distribution shown in Figure 7B. Thus, it was pertinent to determine whether the unliganded AHR_{500} was associated with the same level of XAP2 as AHR_{640} or AHR_{WT}.

Supernatant fractions were prepared from the different cell lines and immunoprecipitation studies carried out as described previously. Figure 7C shows that the level of AHR and XAP2 expression in each of the lines is consistent and that equal amounts of XAP2 can be co-precipitated with the AHR from each of the cell lines regardless of its subcellular localization. Thus, these results confirm that XAP2 can be a component of the unliganded AHR complex when it is localized to the nucleus and suggest that XAP2 does not influence the subcellular localization of the AHR complex when the C-terminal 305 amino acids of the AHR has been removed.

DISCUSSION

The results presented in this report show that endogenous levels of XAP2 can be co-precipitated with the endogenous Ah^{b-1} receptor at time points when the AHR is predominately localized within the nucleus. Indeed, these time course studies suggest that there are several different pools of Ah^{b-1} receptor present in the nucleus of Hepa-1 cells following ligand exposure. These include i) core AHR complexes that remain associated with XAP2, ii) soluble AHRs that are associated with ARNT but not bound to DNA, and iii) AHR•ARNT complexes that are associated with DNA (results not shown, and see Pollenz 1996; Hestermann and Brown 2003). Thus, it appears that XAP2 does not impact the translocation of the Ah^{b-1} receptor to the nucleus after ligand stimulation and support the hypothesis that only a small fraction of the ligand bound AHR actually dimerizes with ARNT during the first 75 minutes of ligand exposure (Pollenz et al., 1999; Pollenz and Dougherty 2005). Interestingly, recent studies suggest that the NLS sequence of the Ah^{b-1} receptor is not masked by the binding of XAP2, but that XAP2 affects AHR localization by perturbing the ability of the NLS domain to actually interact with nuclear import receptors (Petrulis et al., 2003). Thus, the current results suggest that the ligand-binding event is able to overcome the conformational change imposed by the association of the AHR with XAP2.

The association of XAP2 with the Ah^{b-1} receptor in the nucleus may have functional implications in the signal transduction process as it may reduce the ability of the receptor population to form functional dimers with ARNT and bind to DNA. Recent studies support this view by showing that the expression of XAP2 actually reduces the level of gene induction mediated by the Ah^{b-1} receptor (Hollingshead et al., 2004; Pollenz and Dougherty 2005). In addition, the current studies confirm that a soluble pool of Ah^{b-1} receptor complexes can be isolated following extended periods of ligand exposure that remain associated with the same level of XAP2 as unliganded receptors. Since ligand-induced degradation of the AHR appears to require DNA binding (Ma and Baldwin, 2000; Pollenz et al., 2005), the continued association with XAP2 might serve to limit this pool of AHRs from functioning in gene regulation and subsequently being degraded.

Interestingly, previous studies suggest that XAP2 is only associated with 40% of the unliganded Ah^{b-1} receptor complex in Hepa-1 cells (Petrulis et al., 2000). However, results presented in the current report show that overexpression of human XAP2 does not lead to increased levels of endogenous Ah^{b-1} receptor or increased levels of total XAP2 protein associated with the endogenous Ah^{b-1} receptor complex. Indeed, the exogenously expressed hXAP2 appears to replace endogenous mXAP2 in the unliganded Ah^{b-1} receptor complex but does not result in an overall increase in the level of XAP2 immunoprecipitated with the AHR. If only 40% endogenous Ah^{b-1} complexes were associated with XAP2, it would be expected that increased XAP2 expression would drive up the level of XAP2 associated with the AHR complex until it was saturated. Importantly, increased association of XAP2 can be observed when similar studies are carried out in cells that express the mouse Ah^{b-2} receptor since this receptor is associated with 8-10 fold less XAP2 than the Ah^{b-1} receptor under endogenous conditions (Pollenz and Dougherty 2005; RSP unpublished results). In addition, the results presented in the current report show that the relative XAP2:AHR ratio in the core

complex after four hours of ligand exposure is the same as the ratio in the AHR complex precipitated from untreated cells. If XAP2 were associated with only a small population of receptors and involved in stabilization of that population, it would be expected that XAP2:AHR ratio would increase after prolonged ligand exposure since 85% of the population has been degraded. Taken together, these studies support a model in which the majority of the unliganded Ah^{b-1} receptor complexes are associated with XAP2 and this association temporally limits the "transformation" of the receptors following ligand-induced nuclear localization.

The current studies also support a role of endogenous XAP2 in inhibiting the nucleocytoplasmic shuttling behavior of the endogenous Ah^{b-1} receptor but do not support a role for XAP2 in maintaining the unliganded Ah^{b-1} receptor in the cytoplasm of Hepa-1 cells. Indeed, the reduction in endogenous XAP2 by siRNA did not impact the localization of the unliganded Ah^{b-1} receptors and they remained predominantly localized within the cytoplasm. These results are in contrast to those using transient expression models, where the unliganded Ah^{b-1} receptor exhibits a predominantly nuclear localization in the absence of exogenously expressed XAP2 (Kazlauskas et al., 2000; Kazlauskas et al., 2002; Petrulis et al., 2002; Berg and Pongratz 2002). Importantly, when nuclear export was inhibited in Hepa-1 cells that had reduced levels of XAP2, Ah^{b-1} receptors accumulated within the nucleus. These findings are significant because they directly demonstrate that XAP2 is involved in modulating the nuclear import of the unliganded Ah^{b-1} receptor under endogenous conditions. In addition, these results further support a model in which the majority of the unliganded Ah^{b-1} receptor complexes are associated with XAP2 since unliganded Ah^{b-1} receptor complexes do not accumulate in the nucleus when nuclear export was blocked. More importantly however, the results demonstrate that XAP2 is not the sole determinant for whether the unliganded Ah^{b-1} receptor will be localized within the cytoplasmic compartment in the Hepa-1 cell line.

The ultimate subcellular location of a target protein with both NLS and NES domains is related to how it interacts with the nuclear import and export machinery in any given cell (reviewed in Pemberton and Paschal 2005). For example, the AHR_{500} can be detected in the nucleus, even with XAP2 associated, thus in this conformation, nuclear import is clearly favored and the influence of XAP2 in blocking association with import receptors has been diminished. In addition, when the NLS-GFP-GST-NES protein is expressed in Hepa-1 cells, the protein is predominantly localized to the cytoplasm even though the protein is clearly being shuttled through the nucleus and has just as much chance of being predominantly localized there. Thus, it is likely that differences in the association of the Ah^{b-1} receptor with the nuclear import and export machinery can explain the nuclear localization of the Ah^{b-1} receptor in COS cells in the absence of XAP2 (Kazlauskas et al., 2000; Kazlauskas et al., 2002; Petrulis et al., 2002; Berg and Pongratz 2002). In summary, these results show that while XAP2 may modulate the ability of the unliganded Ah^{b-1} receptor to undergo dynamic nucleocytoplasmic shuttling, it does not appear to be the sole determinant of AHR localization in Hepa-1 cells. It is important to note that while XAP2 is ubiquitously expressed in all tissues and cell lines tested to date (Carver and Bradfield 1997; Meyer et al., 1998; Petrulis et al., 2000), it is unclear whether the XAP2:AHR ratio observed in the Hepa-1 cells is the same as that found in tissues. Thus, given the importance of XAP2 as a possible low-penetrance tumor susceptibility gene (Vierimaa et al., 2006), it will be critical to further refine the function of XAP2 in cell culture and tissues, and evaluate its impact on ligand-induced gene regulation mediated by the endogenous Ah^{b-1} receptor as opposed to endogenous AHRs from other species that do not exhibit a high level of association with XAP2.

ACKNOWLEDGMENTS

We are grateful to Dr. Stauber for promptly providing pC3-NLS-GFP-GST-RevNES for these studies. Dr. Gary Perdew is gratefully acknowledged for providing the human XAP2 cDNA expression vectors. Jesal Popat is also acknowledged for excellent technical assistance on some of the experiments.

REFERENCES

Bell DR, Poland A (2000) Binding of aryl hydrocarbon receptor (AhR) to AhR-interacting protein. The role of hsp90. *J Biol Chem*. **275**:36407-36414.

Berg P, Pongratz I (2002) Two parallel pathways mediate cytoplasmic localization of the dioxin (aryl hydrocarbon) receptor. *J Biol Chem*. **277**:32310-32319.

Carver LA, Bradfield CA (1997) Ligand-dependent interaction of the aryl hydrocarbon receptor with a novel immunophilin homolog in vivo. *J Biol Chem*. **272**:11452-11456

Carver LA, LaPres JJ, Jain S, Dunham EE, Bradfield CA. (1998) Characterization of the Ah receptor-associated protein, ARA9. *J Biol Chem*. **273**:33580-33587.

Davarinos NA, Pollenz RS (1999) Aryl hydrocarbon receptor imported into the nucleus following ligand binding is rapidly degraded via the cytosplasmic proteasome following nuclear export. *J Biol Chem*. **274**:28708-28715

Davies TH and Sanchez ER (2005) FKBP52 *Int. J. Biochem. Cell Biol*. **37**, 42-47

Elbi C, Misteli T and Hager GL (2002) Recruitment of dioxin receptor to active transcription sites. *Mol Biol Cell*. **13**:2001-2015

Giannone JV, Okey, AB, and Harper, PA (1995) Charcaterization of polyclonal antibodies to the aromatic hydrocarbon receptor. *Can J. Physiol. Pharmacol*. **7**3:7-17.

Hestermann E, Brown M (2003) Agonist and chemopreventive ligands induce differential transcriptional cofactor recruitment by the aryl hydrocarbon receptor. *Mol Cell Biol* **23**:7920-7925.

Hollingshead BD, Petrulis JR, Perdew GH (2004) The aryl hydrocarbon (Ah) receptor transcriptional regulator hepatitis B virus X-associated protein 2 antagonizes p23 binding to Ah receptor-Hsp90 complexes and is dispensable for receptor function. *J Biol Chem*. **279**:45652-45661

Holmes JL and Pollenz, RS (1997) Determination of aryl hydocarbon receptor nuclear translocator protein concentration and subcellular localization in hepatic and nonhepatic cell culture lines: Development of quantitative western blotting protocols for calculation of aryl hydrocarbon receptor and aryl hydrocarbon receptor nuclear translocator protein in total cell lysates. *Mol. Pharmacol*. **52**:202-211.

Kazlauskas A, Poellinger L, Pongratz I (2000) The immunophilin-like protein XAP2 regulates ubiquitination and subcellular localization of the dioxin receptor. *J Biol Chem*. **275**:41317-41324.

Kazlauskas A, Poellinger L, Pongratz I (2002) Two distinct regions of the immunophilin-like protein XAP2 regulate dioxin receptor function and interaction with hsp90. *J Biol Chem*. **277**:11795-11801.

Knauer SK, Moodt S, Berg T, Liebel U, Pepperkok R and Stauber, RH (2005). Translocation Biosensors to Study Signal-Specific-Nucleo-Cytoplasmic Transport, Protease Activity, and Protein-Protein Interactions. *Traffic* **6**:594-606.

Kudo N, Wolff B, Sekimoto T, Schreiner EP, Yoneda Y, Yanagida M, Horinouchi S, and Yoshida M (1998). Leptomycin B inhibition of signal-mediated nuclear export by direct binding to CRM1. *Exp Cell Res*. **242**:540-547.

Kudo N, Khochbin S, Nishi K, Kitano K, Yanagida M, Yoshida M, and Horinouchi S (1997).Molecular cloning and cell cycle-dependent expression of mammalian CRM1, a protein involved in nuclear export of proteins. *J Biol Chem*. **27**:29742-29751

LaPres JJ, Glover E, Dunham EE, Bunger MK, Bradfield CA (2000) ARA9 modifies agonist signaling through an increase in cytosolic aryl hydrocarbon receptor. *J Biol Chem*. **275**:6153-6159.

Ma Q, Baldwin KT (2000) 2,3,7,8-tetrachlorodibenzo-p-dioxin-induced degradation of aryl hydrocarbon receptor (AhR) by the ubiquitin-proteasome pathway. Role of the transcription activaton and DNA binding of AhR. *J Biol Chem* **275**:8432-8438.

Ma Q, Whitlock JP Jr. (1997) A novel cytoplasmic protein that interacts with the Ah receptor, contains tetratricopeptide repeat motifs, and augments the transcriptional response to 2,3,7,8-tetrachlorodibenzo-p-dioxin. *J Biol Chem*. **272**:8878-8884.

Meyer BK, Perdew GH (1999) Characterization of the AhR-hsp90-XAP2 core complex and the role of the immunophilin-related protein XAP2 in AhR stabilization. *Biochemistry*. **38**:8907-8917.

Meyer BK, Petrulis JR, Perdew GH (2000) Aryl hydrocarbon (Ah) receptor levels are selectively modulated by hsp90-associated immunophilin homolog XAP2. *Cell Stress Chaperones*. **5**:243-254.

Meyer BK, Pray-Grant MG, Vanden Heuvel JP, Perdew GH (1998) Hepatitis B virus X-associated protein 2 is a subunit of the unliganded aryl hydrocarbon receptor core complex and exhibits transcriptional enhancer activity *Mol Cell Biol*. **18**:978-988.

Molinari E, Gilman M, Natesan S (1999) Proteasome-mediated degradation of transcriptional activators correlates with activation domain potency in vivo. *EMBO J.* **18**:6439-6447.

Paine PL, Austerberry CF, Desjarlais LJ and Horowitz SB (1983) Protein loss during nuclear isolation. *J. Cell Biol*. **97**:1240-1242.

Pemberton LF, Paschal BM. (2005) Mechanisms of receptor-mediated nuclear import and nuclear export. *Traffic*. **2005** 6:187-198.

Petrulis JR, Perdew GH (2002) The role of chaperone proteins in the aryl hydrocarbon receptor core complex. *Chem Biol Interact*. **141**:25-40.

Petrulis JR, Hord NG, Perdew GH (2000) Subcellular localization of the aryl hydrocarbon receptor is modulated by the immunophilin homolog hepatitis B virus X-associated protein 2. *J Biol Chem*. **275**:37448-37453.

Pollenz RS and Dougherty EJ (2005) Redefining the role of XAP2 and CHIP in the degradation of endogenous AHR in cell culture models. *J. Biol. Chem* **280**:33346-33356.

Pollenz RS, Santostefano MJ, Klett, E, Richardson VM, Necela B, Birnbaum LS (1998) Female Sprague Dawley rats exposed to a single oral dose of 2,3,7,8-tetrachlorodibenzo-p-dioxin exhibit sustained depletion of aryl hydrocarbon receptor protein in liver, spleen, thymus and lung. *Tox. Sci*. **42**:117-128.

Pollenz RS, Popet J, Dougherty EJ. (2005) Role of the carboxy-terminal transactivation domain and active transcription in the ligand-induced degradation of the mouse Ah^{b-1} receptor. *Biochemical Pharmacology*. **70**:162301633

Pollenz, RS (1996) The aryl hydrocarbon receptor but not Arnt protein is rapidly depleted in hepatic and non hepatic culture cells exposed to 2,3,7,8-tetrachlorodibenzo-p-dioxin. *Mol. Pharmacol*. **49**:391-398

Pollenz RS, Sattler CA, Poland A (1994) The aryl hydrocrabon receptor and aryl hydrocrabon receptor nuclear translocator protein show distinct subcellular localization in Hepa 1c1c7 cell by immunofluorescence microscopy. *Mol Pharmacol*. **45**:428-438.

Ramadoss P, Petrulis JR, Hollingshead BD, Kusnadi A, Perdew GH. (2004) Divergent roles of hepatitis B virus X-associated protein 2 (XAP2) in human versus mouse Ah receptor complexes. *Biochemistry*. **43**:700-709.

Song Z, Pollenz RS (2002) Ligand dependent and independent modulation of AH receptor localization, degradation, and gene regulation. *Mol. Pharmacol* **62**:806-816

Vierimaa O, Georgitsi M, Lehtonen R, Vahteristo P, Kokko A, Raitila A, Tuppurainen K, Ebeling TM, Salmela PI, Paschke R, Gundogdu S, De Menis E, Makinen MJ, Launonen V, Karhu A, Aaltonen LA. (2006) Pituitary adenoma predisposition caused by germline mutations in the AIP gene *Science* **312**:1228-1230

FOOTNOTES

This work was supported in part by NIH grant # ES10991 to RSP. Portions of this work were presented at the Society of Toxicology Annual Meeting 2006.

Reprint requests to: Richard S Pollenz, University of South Florida, Department of Biology, BSF 110, 4202 E Fowler Ave, Tampa, FL 33620, Tel. 813-974-1596, Fax. 813-974-3263, E-Mail:pollenz@cas.usf.edu

FIGURE LEGENDS

Figure. 1. Analysis of AHR localization and degradation in Hepa-1 cells. A) Hepa-1 cells were grown on glass coverslips and exposed to me_2SO (0.1%) for 300 minutes (time = 0) or TCDD (2nM) for the indicated times. Cells were fixed and then incubated with A-1 IgG (1.0µg/ml) and visualized with GAR-RHO IgG (1:400). All panels were photographed under identical exposures. Bar = 10µ. Numbers represent TCDD exposure times in minutes. **B)** Nuclear fluorescence intensities were determined for the cells presented in A. 50-75 cells in 3-4 distinct fields of view were quantified using MicroSuite image analysis software and the average +/-SE plotted as relative pixel density vs. time. The level of AHR and actin protein shown in C was determined by computer densitometry as detailed in Materials and Methods. Normalized values are plotted as the average +/- SE three individual samples. * = statistically different from time 0 samples, $p > .005$. **C)** Triplicate plates of Hepa-1 cells were exposed to me_2SO (0.1%) for 300 minutes (time = 0) or TCDD (2nM) for the indicated times. Equal amounts of total cell lysates were then resolved by SDS-PAGE, blotted and stained with A-1A IgG (1.0µg/ml) and ß-actin IgG (1:1000). Reactivity was visualized by ECL with GAR-HRP IgG (1:10,000) and bands quantified and normalized as detailed.

Figure 2. Association of endogenous AHR, ARNT and XAP2 in Hepa-1 cells treated with TCDD. A) Cytosol was prepared from Hepa-1 cells treated with either me_2SO (0.1%) for 75 minutes or TCDD (2nM) or for 20, 40, 60 or 75 minutes. 600µg of cytosol from each time point was then precipitated with either AHR (AHR-IgG) or pre-immune IgG (Pi-IgG) as detailed in *Materials and Methods*. Each of the precipitated samples as well as 15µg cytosol (input) was resolved by SDS-PAGE and blotted. Blots were stained with either A-1A IgG (1.0µg/ml), R-1 IgG (1.0µg/ml) or XAP2 mouse IgG_1 (1:750) and reactivity visualized by ECL with GAR-HRP or GAM-HRP IgG (1:10,000).

The IgG bands are presented to show the consistency of the precipitations. **B)** Computer densitometry was used to determine the relative level of AHR, ARNT or XAP2 protein present in the precipitated samples presented on the blot in (A). Each bar represents the relative densitometry units of an individual band and can be used to evaluate differences in the ratio of XAP2:AHR or ARNT:AHR in the different samples. However, due to the difference in the sensitivity of each antibody for its target protein, the ratio does not represent the absolute number of protein molecules. **C)** Cytosol was prepared from Hepa-1 cells treated with either me_2SO (0.1%) or TCDD (2nM) for 4 hrs. 600µg of control (0) and 4.2mg of 4 hr cytosol (4) was precipitated as described in (A). The precipitated samples as well as 15µg cytosol (input) was resolved by SDS-PAGE, blotted and the identical samples stained for either AHR or XAP as detailed above. Ah: precipitated with A-1A (AHR) IgG; Pi: precipitate with pre-immune rabbit IgG. **D)** Computer densitometry was used to determine the relative level of AHR and XAP2 protein present in the precipitated samples as described in (B). Ah: relative level of AHR protein. mX: relative level of XAP2 protein. Note that the relative ratio of XAP2:AHR is unchanged in the 4 hr samples compared to the controls.

Figure 3. Localization of endogenous Ah^{b-1} receptor in Hepa-1 cells expressing hXAP. Hepa-1 cells were transfected with pCI-hXAP2 along with FITC labeled RNA (BLOCK-IT®), pEYFP-XAP2-FLAG, or control vector pCDNA3.1 as detailed in *Materials and Methods.* After 24 hrs, populations of cells were either harvested for the generation of total cell lysates, or fixed for Immunocytochemical staining. **A)** Equal amounts of the indicated samples were resolved by SDS-PAGE and blotted. Blots were stained with either A-1A IgG (1.0µg/ml), XAP2 mouse IgG_1 (1:750) or anti-actin IgG (1:1000) and reactivity visualized by ECL with GAR-HRP or GAM-HRP IgG (1:10,000). Con = cells transfected with pcDNA3.1. +XAP = cells transfected with pCI-hXAP2 and BLOCK-IT®. +Y-XAP = cells transfected with pEYFP-hXAP2-FLAG. **B)** The exact Hepa-1

populations that were transfected as detailed in (A) were fixed and stained for the AHR with A-1 IgG (1.0µg/ml) and visualized with GAR-RHO IgG (1:400). Con AHR = AHR staining pattern in cells transfected with pcDNA3.1. AHR + hXAP2 = AHR staining pattern in cells transfected with pCI-hXAP2 and BLOCK-IT®. FITC = FITC labeling of the exact field presented to the left to illustrate the transfection efficiency of the experiment. YFP-XAP2 = pattern of the expressed EYFP-XAP2-FLAG. AHR = AHR staining pattern of the exact field presented to the left. The arrows indicate cells that are not expressing the EYFP-XAP2-FLAG protein. Bar = 10µ.

Figure 4. Association of endogenous XAP2 with AHR in Hepa-1 cells transfected with hXAP expression vectors. Hepa-1 cells were transfected with pCI-hXAP2 or control vector pcDNA3.1 as detailed in *Materials and Methods.* After 24 hrs, populations of cells were harvested cytosol generated for immunoprecipitation experiments. **A)** 600µg of cytosol from the indicated samples were precipitated in duplicate with either AHR (AHR-IgG) or pre-immune IgG (Pi-IgG) as detailed in *Materials and Methods*. Each of the precipitated samples as well as 15µg cytosol (input) was resolved by SDS-PAGE and blotted. Blots were stained with either A-1A IgG (1.0µg/ml) or XAP2 mouse IgG_1 (1:750) and reactivity visualized by ECL with GAR-HRP or GAM-HRP IgG (1:10,000). Endogenous mouse XAP2 (mXAP2), exogenous human XAP2 (hXAP2) and AHR indicated AHR. The IgG bands are presented to show the consistency of the precipitations. C = samples from cells transfected with pcDNA3.1. X = samples from cells transfected with pCI-hXAP2. **B)** Computer densitometry was used to determine the relative level of AHR or XAP2 protein present in the precipitated samples presented on the blot in (A). Each bar represents the relative densitometry units of an individual band and can be used to evaluate differences in the ratio of XAP2:AHR in the different samples. However, due to the difference in the sensitivity of each antibody for its target

protein, the ratio does not represent the absolute number of protein molecules. Note that the XAP2:AHR ratio is essentially unchanged in all the samples.

Figure 5. Reduction of endogenous XAP2 by siRNA knock down and analysis of nucleocytoplasmic shuttling in Hepa-1 cells. A) Hepa-1 cells were transfected with siRNA specific to XAP2 or control siRNA as detailed in *Materials and Methods*. 48 hrs later, cytosol was prepared and 600µg precipitated with either AHR (Ah-IgG) or pre-immune IgG (Pi-IgG) as detailed in *Materials and Methods*. Each of the precipitated samples as well as 15µg cytosol (input) was resolved by SDS-PAGE and blotted. Blots were stained with either A-1A IgG (1.0µg/ml) or XAP2 mouse IgG_1 (1:750) and reactivity visualized by ECL with GAR-HRP or GAM-HRP IgG (1:10,000). The IgG bands are presented to show the consistency of the precipitations. C: cells transfected with control siRNA; X: cells transfected with XAP2 siRNA. **B)** Computer densitometry was used to determine the relative level of AHR or XAP2 protein present in the precipitated samples presented on the blot in (A). Each bar represents the relative densitometry units of an individual band and shows that the ratio of XAP2:AHR has changed in the siXAP samples. Ah: level of AHR protein. mX: level of XAP2 protein. **C)** Hepa-1 cells were transfected with pC3-NLS-GFP-GST-RevNES and allowed to recover for 24 hrs. Cells were treated with either methanol (0.1%) of LMB (1nM) for 2 hrs and the live cells visualized by fluorescence microscopy. Bar = 10µ.

Figure 6. Subcellular localization of AHR in cells with reduced levels of XAP2. Hepa-1 cells were transfected with siRNA specific to XAP2 or control siRNA along with FITC labeled RNA (BLOCK-IT) as detailed in *Materials and Methods.* 48hrs later cells were treated with either methanol (0.1%) of LMB (1nM) for 4 hrs and either fixed for immunofluorescence microscopy or harvested for the preparation of total cell lysates. **A)** Western blot of AHR and XAP2 expression in total cell lysates prepared from cells transfected with control siRNA (siCON) or XAP2 siRNA (siXAP). **B)** Cells visualized for

AHR. Fixed cells were stained with A-1 IgG (1.0µg/ml) and visualized with GAR-RHO IgG (1:400). The FITC labeled panels represent the exact fields presented to the left and illustrate the transfection efficiency of the experiment. Bar = 10µ.

Figure 7. Localization of AHRs containing C-terminal truncations. A) Schematic of the AHR truncations used in the experiments. b: basic region; HLH: helix-loop-helix; PAS: Per-ARNT-Sim domain. Numbers represent amino acids. **B)** The indicated cell lines were fixed and stained with A-1 IgG (1.0µg/ml) and visualized with GAR-RHO IgG (1:400). Bar = 5µ. **C)** Cytosol was prepared from the indicated cell lines and 600µg precipitated with either AHR (Ah-IgG) or pre-immune IgG (Pi-IgG) as detailed in *Materials and Methods*. Each of the precipitated samples as well as 15µg cytosol (input) was resolved by SDS-PAGE and blotted. Blots were stained with either A-1A IgG (1.0µg/ml) or XAP2 mouse IgG_1 (1:750) and reactivity visualized by ECL with GAR-HRP or GAM-HRP IgG (1:10,000). 640 = AHR_{640} cell lines; 500 = AHR_{500} cell line; WT = AHR_{WT} cell line; LA = LA-I cell line.

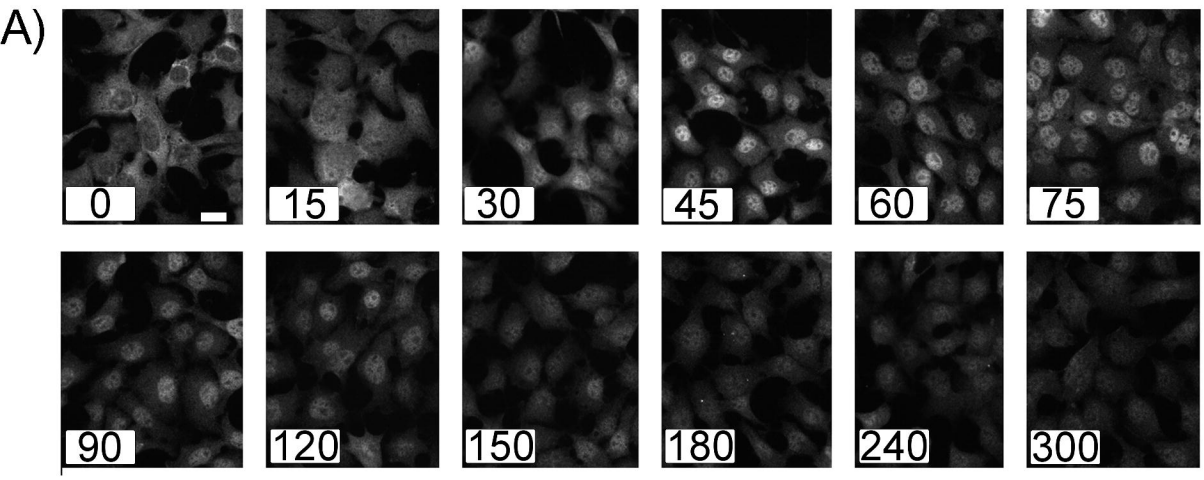
A)
0
15
30
45
60
75
90
120
150
180
240
300

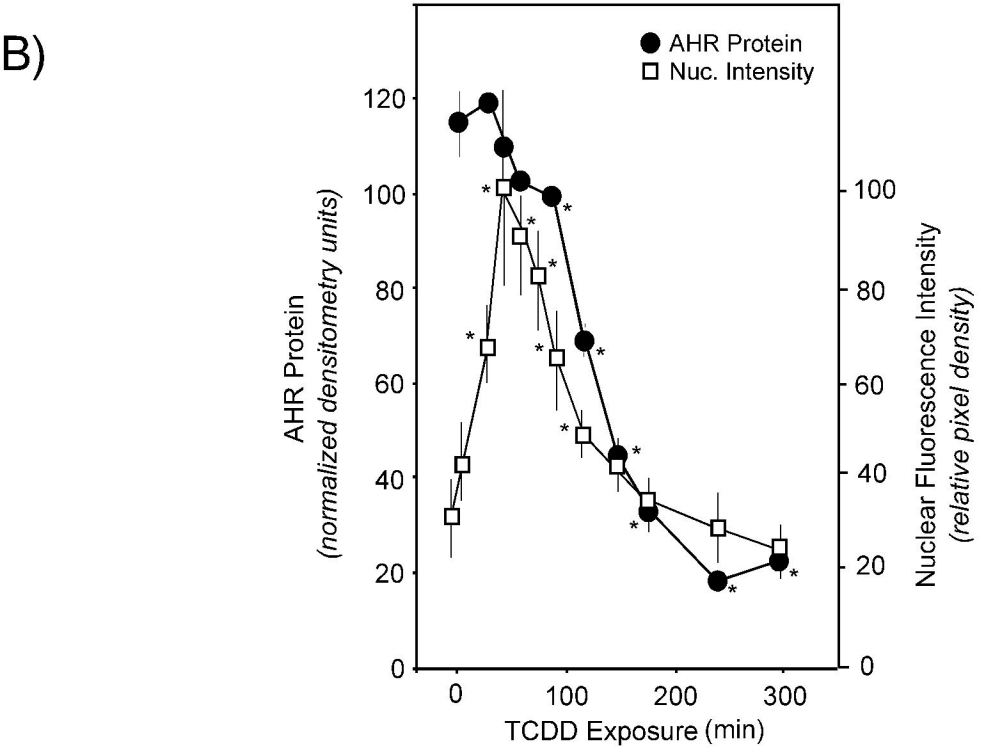
B)
AHR Protein
Nuc. Intensity
AHR Protein
(normalized densitometry units)
Nuclear Fluorescence Intensity
(relative pixel density)
TCDD Exposure (min)
0
20
40
60
80
100
120
0
100
200
300

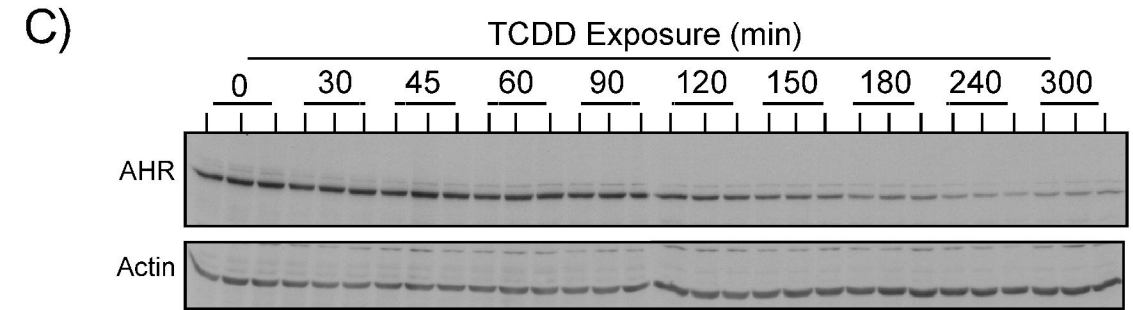
C)
TCDD Exposure (min)
0
30
45
60
90
120
150
180
240
300
AHR
Actin

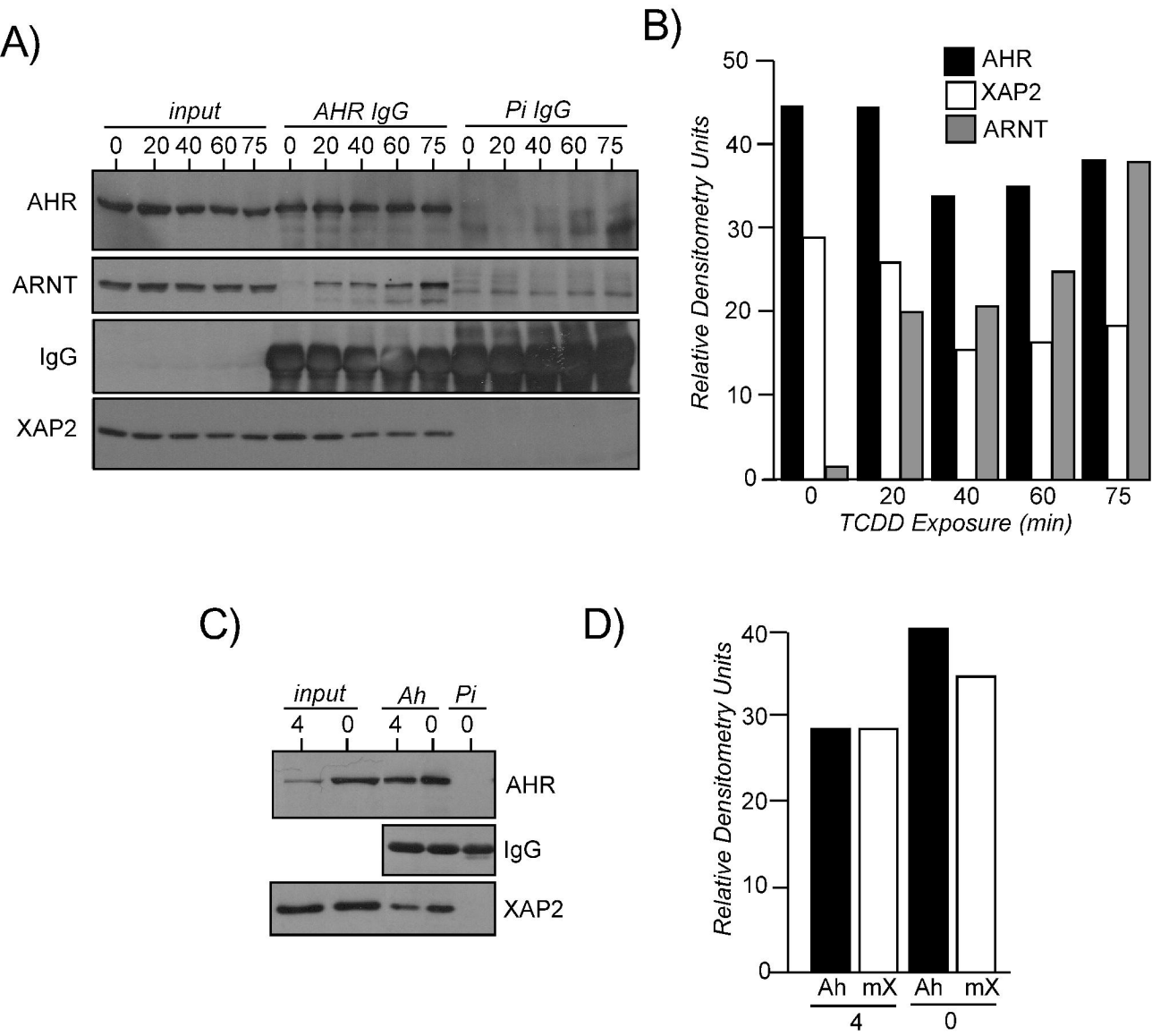
A)
input
AHR IgG
Pi IgG
0 20 40 60 75 0 20 40 60 75 0 20 40 60 75
AHR
ARNT
IgG
XAP2
B)
AHR
XAP2
ARNT
Relative Densitometry Units
50
40
30
20
10
0
0 20 40 60 75
TCDD Exposure (min)
C)
input
Ah
Pi
4 0 4 0 0
AHR
IgG
XAP2
D)
Relative Densitometry Units
40
30
20
10
0
Ah mX Ah mX
4 0

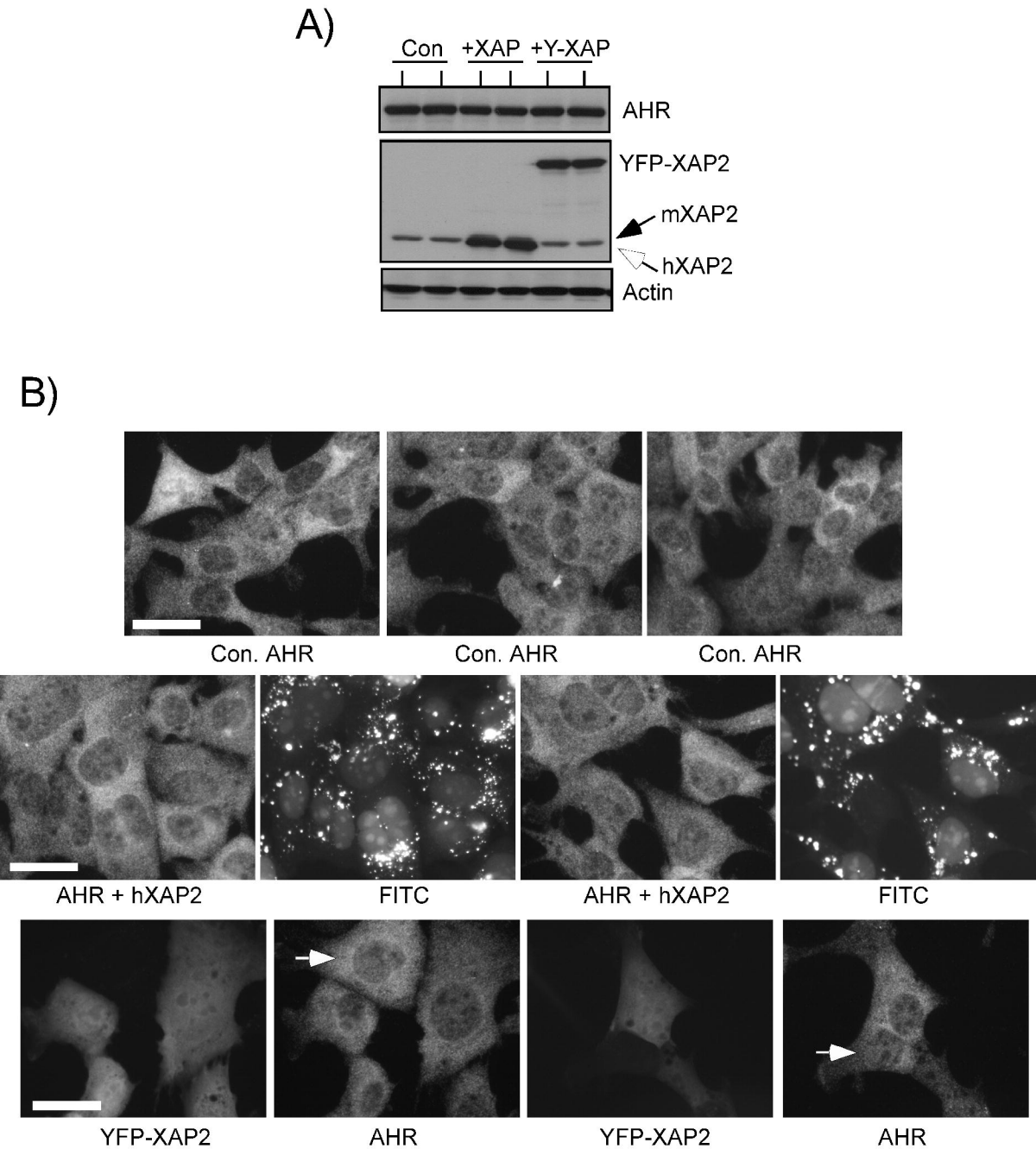
A)
Con
+XAP
+Y-XAP
AHR
YFP-XAP2
mXAP2
hXAP2
Actin
B)
Con. AHR
Con. AHR
Con. AHR
AHR + hXAP2
FITC
AHR + hXAP2
FITC
YFP-XAP2
AHR
YFP-XAP2
AHR

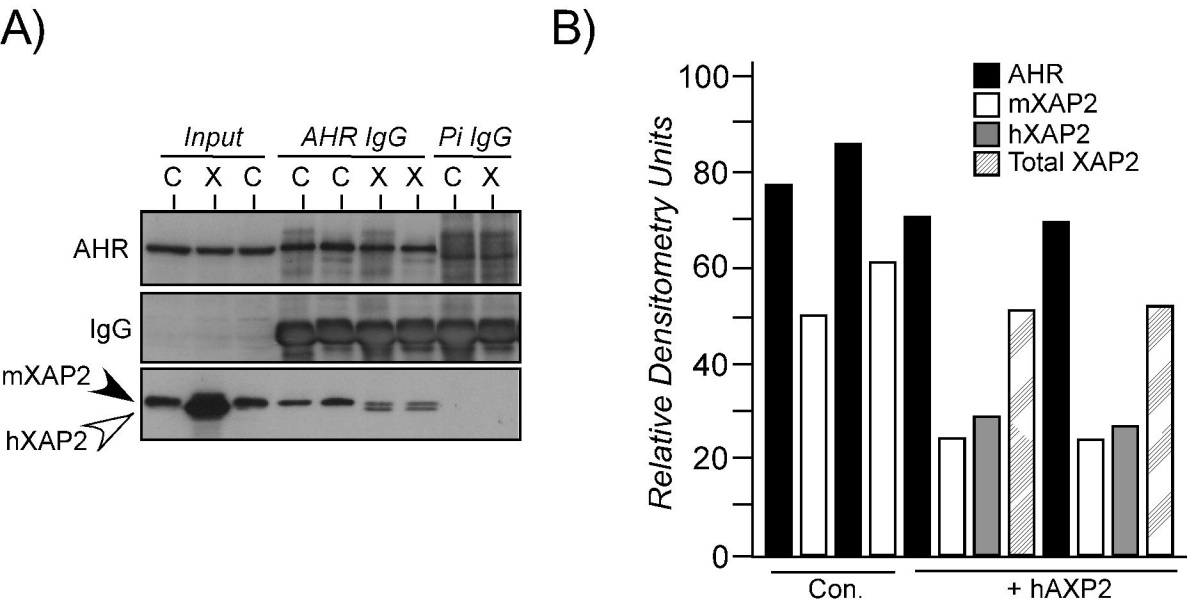
A)
Input
AHR IgG
Pi IgG
C X C C C X X C X
AHR
IgG
mXAP2
hXAP2
B)
Relative Densitometry Units
100
80
60
40
20
0
AHR
mXAP2
hXAP2
Total XAP2
Con.
+ hAXP2

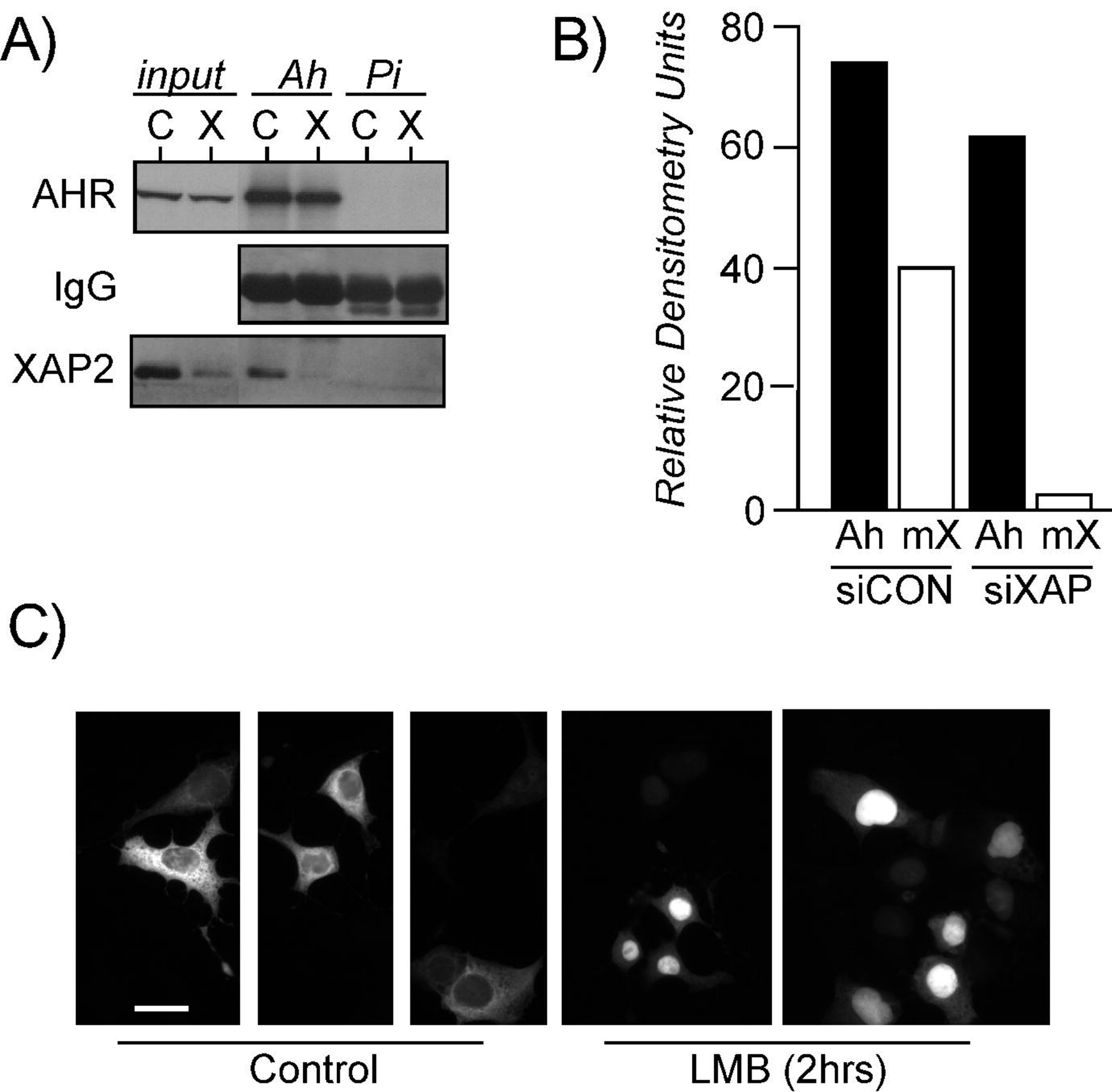
A)
input
Ah
Pi
C X C X C X
AHR
IgG
XAP2
B)
Relative Densitometry Units
80
60
40
20
0
Ah mX Ah mX
siCON siXAP
C)
Control
LMB (2hrs)

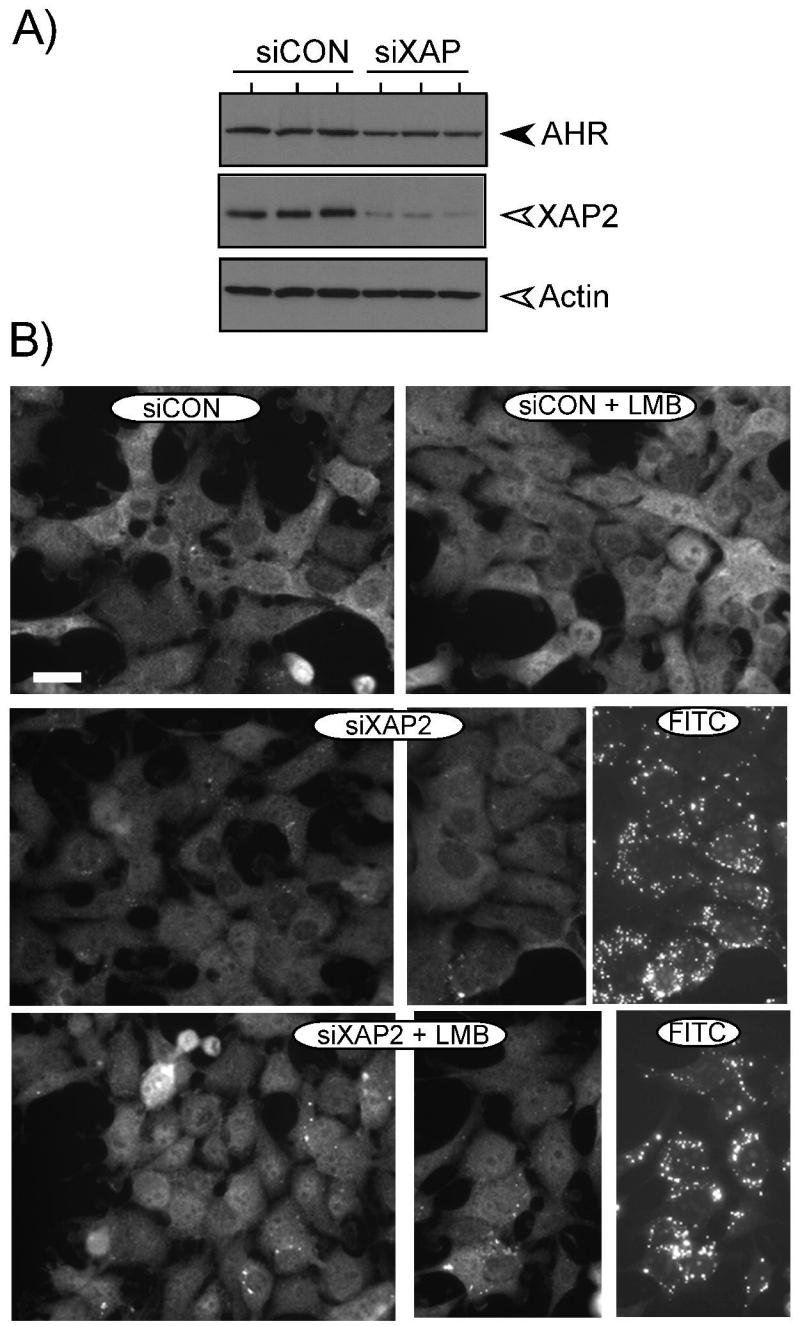
A)
siCON
siXAP
AHR
XAP2
Actin
B)
siCON
siCON + LMB
siXAP2
FITC
siXAP2 + LMB
FITC

A)

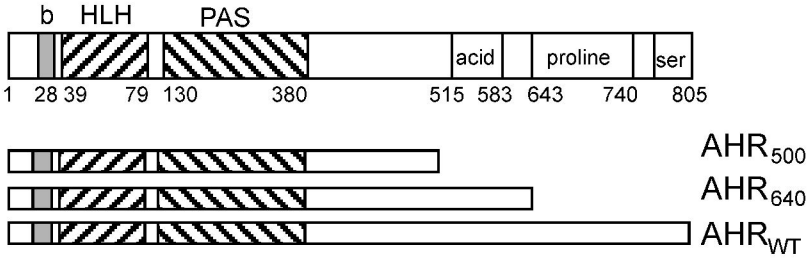
b
HLH
PAS
acid
proline
ser
1
28
39
79
130
380
515
583
643
740
805
AHR500
AHR640
AHRWT

B)

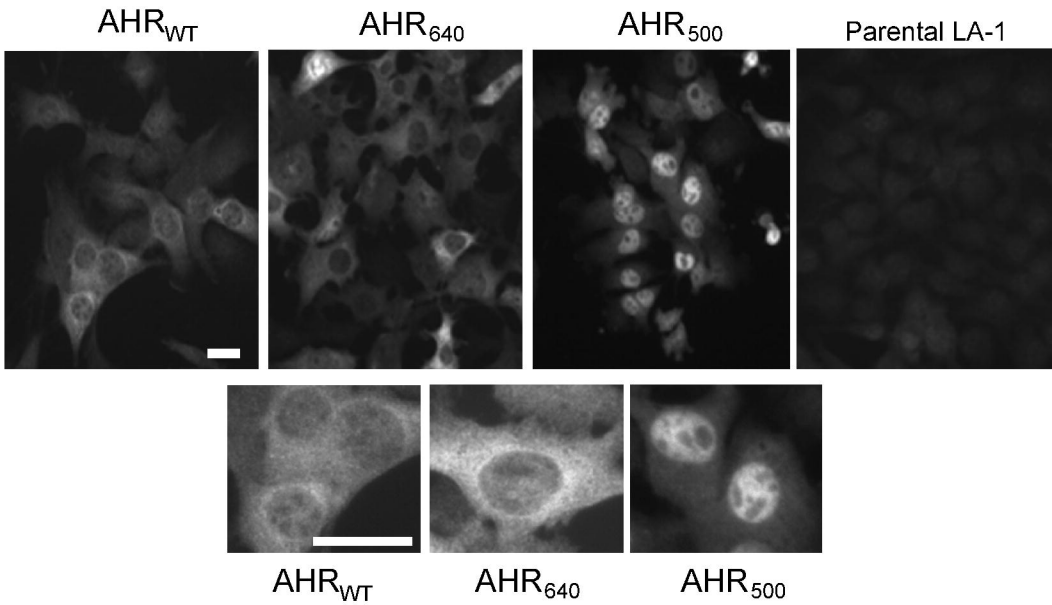
AHRWT
AHR640
AHR500
Parental LA-1
AHRWT
AHR640
AHR500

C)

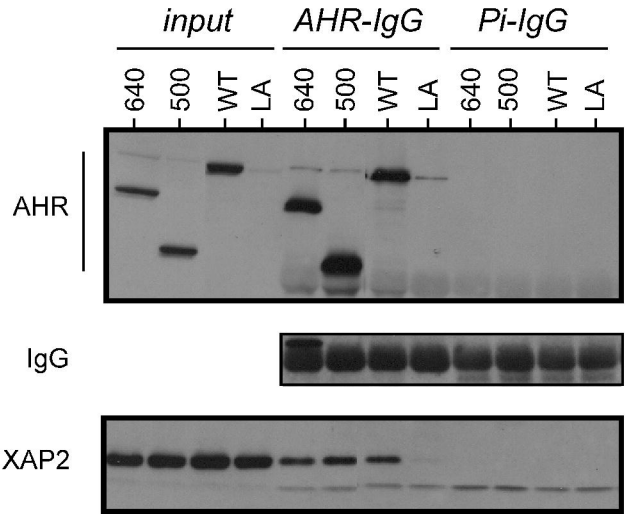
input
AHR-IgG
Pi-IgG
640
500
WT
LA
AHR
IgG
XAP2